JOURNAL OF PROPULSION AND POWER
Vol 8, No. 2, March–April 1992

Evaluation of Parallel Injector Configurations for Mach 2 Combustion

G. Burton Northam*
NASA Langley Research Center, Hampton, Virginia 23665
I. Greenberg† and C. S. Byington‡
George Washington University, Hampton, Virginia 23665
and
D. P. Capriotti§
Analytical Services and Materials, Hampton, Virginia 23665

An experimental study of wall-mounted parallel injector ramps has been conducted to explore techniques to enhance mixing in a scramjet combustor. Downstream parallel injection may be useful at high speeds to extract thrust from hydrogen that has been used to cool the engine and the airframe. The swept ramp fuel injector employed here should produce vortex shedding and local separation (like a rearward-facing step), which should enhance mixing. Perpendicular fuel injectors were added downstream of the swept ramps to determine if the vortical wake flow generated by the parallel injectors—with no fuel injection—is effective in enhancing the mixing of the transverse fuel jet. For performance comparisons, an unswept, but otherwise identical, parallel injector was also tested. The injector ramps were designed to yield a reflected shock wave from the duct top wall such that it passed just downstream of the barrel shock of the fuel injectors. The Mach number at the exit of the fuel injector was designed to be 1.7 to produce an underexpanded fuel flow under almost all operating conditions. Direct-connect tests were conducted with a vitiated heater over a total temperature range. Flow visualization tests with an unducted freejet configuration were conducted using shadowgraph and ultraviolet television camera systems for OH radical visualization. Three duct configurations were tested. Tests of the swept ramp with a 100-mm constant-area duct downstream of the injector block resulted in upstream interaction at almost any equivalence ratio. Increasing the duct expansion rate allowed the equivalence ratio to be increased beyond 1.5 with rapid mixing and combustion over a wide total temperature range. The unswept ramp design resulted in lower combustion efficiency and a sensitivity of efficiency to heater total temperature, or duct velocity.

Nomenclature

G	= gap, mm
$M1$	= Mach number of the flow at the exit of the heater nozzle
MEH	= fuel injection Mach number
$P0$	= average measured static pressure at the exit of the nozzle, kPa
$P2$	= static pressure behind the shock wave generated by the ramps, kPa
PH	= static pressure of the fuel at the exit of the parallel injector, kPa
PHI, ϕ	= fuel-air equivalence ratio
P_{heater}	= total pressure in the heater, kPa
TT	= heater total temperature, K
$V2$	= flow velocity behind the oblique shock wave, m/s
X	= distance, mm
$X1$	= distance for complete fuel-air mixing when $\phi = 1$, mm
X_ϕ	= distance for complete fuel-air mixing, mm
γ	= specific heat ratio
$ETAC$, η_c	= calculated combustion efficiency
η_m	= fuel-air mixing efficiency
ϕ_r	= reacted fuel-air equivalence ratio
ϕ_t	= total fuel-air equivalence ratio

Presented as Paper 89-2525 at the AIAA/ASME/SAE/ASEE 25th Joint Propulsion Conference, Monterey, CA, July 10–12, 1989; received Aug. 21, 1989; revision received June 10, 1990; accepted for publication Sept. 21, 1990.

*Group Leader, Experimental Methods Branch. Member AIAA.
†Visiting Scientist, Joint Institute for the Advancement of Flight Sciences; currently at RAFAEL, Haifa, Israel. Member AIAA.
‡Research Associate, Hypersonic Propulsion Branch, Joint Institute for the Advancement of Flight Sciences; currently, Research Engineer, ARL, Pennsylvania State University, University Park, PA 16804. Member AIAA.
§Research Engineer. Member AIAA.

Introduction

EXPERIMENTAL and theoretical studies are being conducted to explore techniques to enhance mixing for scramjet combustion.[1] The Hypersonic Propulsion Branch at NASA's Langley Research Center has used perpendicular and parallel fuel injection to control the mixing distribution in subscale scramjet engine simulated tests at Mach 4 and 7 simulated flight conditions.[2-4] With increased emphasis on the higher flight Mach numbers required for vehicles like the National Aerospace Plane, exploration of techniques to en-

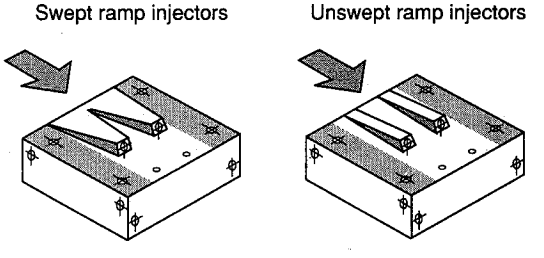

Fig. 1 Injector blocks.

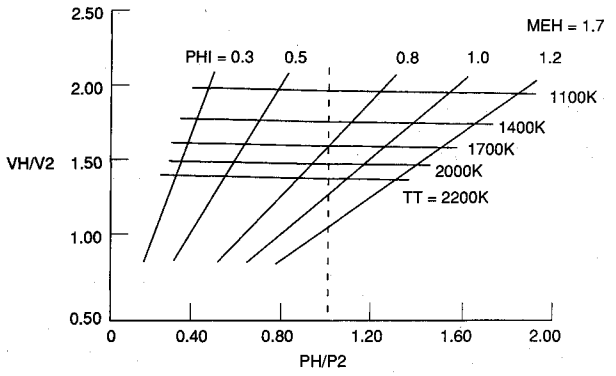

Fig. 2 Variation of flow parameters.

hance mixing and thus reduce the combustor length have become essential to a successful program. Since downstream parallel injection may be useful at high speeds to extract energy from hydrogen that has been used to cool the engine and the airframe, techniques to enhance the relatively slow mixing associated with parallel injection are being investigated. As part of this investigation, a series of tests with wall-mounted parallel injectors were conducted with hydrogen injected at Mach 1.7 from the base of ramps that were inclined 10.3 deg to the combustor wall. At the front of the injector block, the ramp in the first series of tests extended all of the way across the duct and resulted in a two-dimensional reflected wave crossing the injected fuel just downstream of the apex of the ramp. The side walls of the two ramps were swept at 80 deg and ended in a nearly square base (15.2 mm on a side) from which the fuel was injected through a conical nozzle. The swept ramp injector configuration was intended to induce vortical flow and local recirculation regions similar to the rearward-facing step that has been used for flameholding in supersonic flow. The 12% blockage is approximately the same projected area used in most studies that utilize rearward-facing steps as flameholders. The interaction of the reflected shock with the lower density fuel jet should also result in increased mixing.[5-8]

As pointed out by Swithenbank,[9] there is probably some optimum trade between the pressure losses induced by the fuel injection and mixing augmentation process and the resulting increase in combustion efficiency. Of course, these losses become more pronounced at the higher Mach numbers. The pressure rise in the base region of the swept ramp injectors offers some opportunity to reduce these losses.

The swept ramp injector design was evaluated in several expanding duct configurations with increasing area ratios. Since previous results with parallel injection from a strut had indicated slower mixing than transverse injection, a constant area section was added downstream of the swept ramp injectors to aid mixing and maintain pressure to insure combustion. This constant-area section was not required with the swept ramp injectors. During the test program, the area ratio and the rate of expansion were increased and combustion was maintained. Also, during the latter stages of the test program an unswept ramp injector block was constructed. This unswept ramp model was tested for comparison with the swept configuration.

The design of the injector blocks, the test procedure, the results from open duct tests, and lastly the combustion tests are discussed in the following sections.

Ramp Injector Design

Two injector blocks (Fig. 1) were designed for the investigation of mixing enhancement techniques with parallel injection. The first model was swept with respect to the streamwise direction, whereas the sidewalls of the second model were machined to be parallel with the oncoming flow. The main design parameters, the ramp angle and the injection Mach number, were determined for the swept ramp injector at Mach 2 freestream conditions using basic gas dynamic relations.[10] Identical ramp angles and fuel nozzle configurations were used for both designs. Since Ref. 1 presents a thorough review of the design, only an overview is presented here.

The injector ramp angle and percent area blockage were the main design criteria to be determined for the ramp geometry. The flow obstruction must be minimized to prevent the formation of large subsonic pockets and maintain fully supersonic flow. Moreover, the ramp must be at an angle that produced a reflected oblique shock that cleared the apex of the ramp yet also effectively interacted with the fuel jet to promote mixing. With these objectives in mind, the ramp angle and area blockage were chosen as 10.3 deg and 11.5%, respectively.

The fuel injector Mach number was designed based upon heater and injector conditions. The Mach number was chosen as 1.7, since it resulted in an underexpanded jet of gaseous hydrogen for the broadest range of fuel equivalence ratios and heater total temperatures (Fig. 2). The nozzle diameter of the parallel fuel injector was 7.11 mm for this Mach number. It should be noted that, due to the nature of an underexpanded jet, the flow will continue to expand (or plume) as it exits the nozzle. This expansion tends to lessen the importance of the exit area ratio on the jet characteristics and increase the dependence on the jet nozzle throat area (sonic point) and total pressure. Again, for further elaboration on the design considerations, see Ref. 1.

Apparatus

Test Facility

The study was conducted in test cell 2 at the Hypersonic Propulsion Branch, NASA Langley Research Center. The high enthalpy test gas required to simulate scramjet combustor flow was produced by a hydrogen-oxygen-air burner. The flow rates of air, hydrogen, and oxygen were varied to achieve the desired total temperatures, pressures, and free oxygen content. The heater total temperatures ranged from 1400 to 2200 K (± 5%). The total pressure was 795 kPa (± 5%). These conditions yielded a static pressure at the exit of the Mach 2 nozzle of approximately 101 kPa, or 1 atm. The oxygen content of the vitiated air was monitored throughout the tests. Only those tests in which the vitiated air contained 20.95 (± 1) percent oxygen by volume were used for further analysis. An air ejector was connected to the aft end of the diverging combustor duct to prevent atmospheric back pressure from influencing combustor performance. Ejector flow

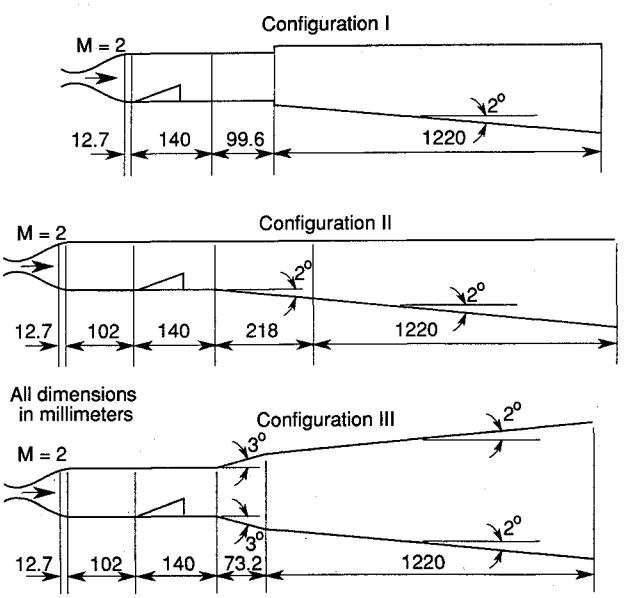

Fig. 3 Duct configurations.

rate was set such that the pressure at the end of the combustor duct was approximately 51 kPa, or 0.5 atm. Flow rates in the test were measured using orifice plates. A programmable controller was used in the tests to trigger various events related to fuel injection timing.

Duct Configurations

Direct-connect tests were conducted with different expansion duct configurations. An open-duct test was first conducted for flow visualization, and three duct configurations were tested for combustor performance analysis (Fig. 3).

Open Duct

To achieve flow visualization, the swept ramp injector block was mounted without the side walls to provide optical access. A collection duct was located about 50 mm from the block to catch the hot gases and prevent expansion in the test cell.

Duct Configuration I

The heater nozzle ended with a 12.7 mm-thick rectangular flange instrumented with pressure taps to measure combustor inlet or nozzle exit wall pressures. The swept ramp injector block (140 mm long) was attached to this flange and mounted with top and side walls. A constant area duct, 98.6 mm long and 87.9 × 38.4 mm in cross section, was connected to the injector model. This was followed by a 1.22 m-long expansion duct. This duct had a straight upper wall and a 2 deg divergence on the bottom wall. Its entrance cross section was 87.9 × 45.7 mm, which resulted in a step at the interface with the constant-area duct. This rearward-facing step was used as a flameholding region to promote complete combustion. However, this step was unnecessary and, along with the lack of an isolator, agitated the upstream interaction problem.

Duct Configuration II

In this configuration, a constant area duct was mounted upstream to provide an isolator section 102 mm long. The expansion duct was attached to the end of the injector block, had a straight upper wall and diverged 2 deg along the bottom wall (see Fig. 3). A short 2 deg expansion duct was constructed to interface the injector block to the existing 1.22 m-long duct without a step. Only the swept ramp injector block was tested with this configuration.

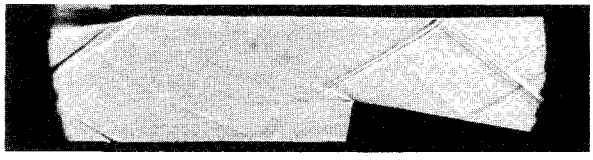

a) No fuel injection

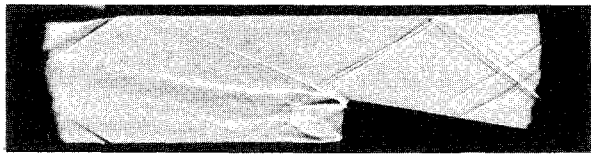

b) Parallel injection, *PHI* = 0.90

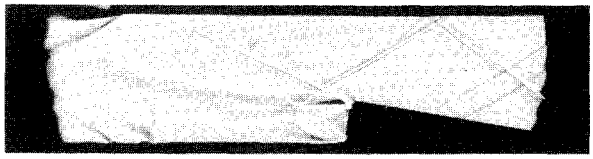

c) Parallel injection, *PHI* = 0.90 combined with perpendicular injection, *PHI* = 0.13

Fig. 4 Shadowgraphs, *TT* = 1700 K, P_{heater} = 800 kPa.

Duct Configuration III

This configuration was similar to configuration II, but featured a more immediate and greater expansion directly downstream of the injector block. The expansion duct was assembled from two sections: a 3 deg divergent (both walls), 73.2 mm-long duct, and a 2 deg divergent (both walls), 1.22 m-long duct (see Fig. 3). Both the swept and unswept ramp injectors were tested with this duct configuration.

Data Acquisition

The data taken during each test was divided into two major groups. The first group contained the facility parameters and was permanently recorded for all the tests. A total of 30 measurement channels were used.

The second group contained pressures located along the model walls and the expansion duct, and were measured by an electronic scanning pressure (ESP) system. A total of 140–160 channels were utilized, depending on the configuration. In each test, the data were converted to engineering units in near real-time for evaluation of a test, and stored on a PC hard drive for future analysis. Plots of pressure distribution in the duct and in the injector block section were provided immediately after the test to evaluate combustor performance parameters, such as upstream interaction and pressure ratio. Data measurement frequency was 10 Hz and display frequency was 2 Hz.

Shadowgraphs System and UV-TV Camera Setup

Initial flow visualization tests were monitored by two systems: Shadowgraphs located perpendicular to the duct axis and focused on the injector block (open-duct tests). The shadowgraph was photographed by a high-speed camera and recorded using a video cassette recorder (VCR). Ultraviolet television (UV-TV, 310 nm) camera was located approximately 80 deg to the flow axis and was used to monitor OH emission. The results were recorded on a VCR cassette. Two VCRs and monitors were located in the control room to observe and record the open-duct tests.

Test Procedures

The fuel equivalence ratio and total temperature were varied such that a matrix of performance information could be obtained for several combinations of fuel injector types and duct configurations.

Open-Duct Tests

Within 2 s of the heater's transient startup, the data acquisition system, shadowgraph system, UV-TV camera, and VCR's were activated; 3 s later, fuel was injected from the parallel injectors; 5 s later, perpendicular fuel injection was added. After approximately five more seconds, fuel to the model was turned off. The cameras and data acquisition system were turned off. Then the hydrogen and oxygen flows to the heater were terminated to complete the test. The data received were evaluated in near real-time. Based on these results, a change in fuel supply pressure for a different equivalence ratio or change in heater total temperature was made.

Duct Configuration Tests

Basically, the test procedure for all duct configuration tests was similar. The main differences were in the timing and combinations of fuel injection. About 3 s after the transient startup of the facility heater, the parallel fuel was turned on; 5 s later, perpendicular fuel injection was added; 2 s later, the parallel fuel was turned off, and after an additional 3 s, the perpendicular fuel was turned off. In the runs with duct configuration III, the parallel and perpendicular injection were

turned off simultaneously. For total temperatures of 2000 K and above, the fuel injection duration time was shortened. For this reason, the overall run time was about 8 s instead of 12 s.

Data Analysis Procedure

1) Two data files were received for each test. The first one included all the facility data, and the second included the ESP duct wall pressures.

2) From the hard copy, received in near real-time, cycles were chosen to be analyzed. Typically, two cycles from each batch were analyzed. In the first, only the parallel injection was on, and, in the second, both parallel and perpendicular injection were on. For some runs, the second cycle was analyzed for perpendicular injection only. Test cycles in which upstream interaction was observed were not analyzed for combustor performance. For each total temperature, a cycle with no fuel injection was chosen for reference conditions.

3) The test output data were formatted compatible with the input data file for the one-dimensional analysis program. The pressure distribution in this file was obtained from the average pressures measured at each duct cross-section.

4) Data files were transferred to the NASA Langley computer system.

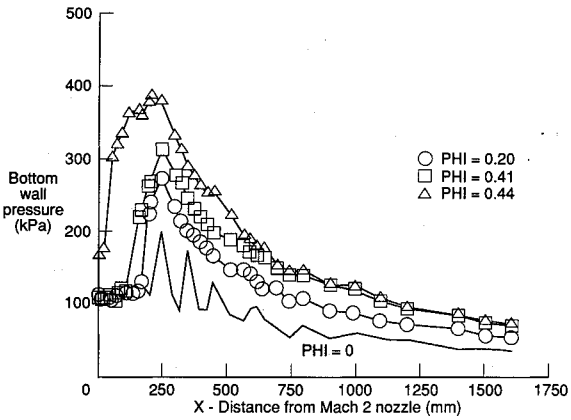

a) Swept ramp injector—configuration II, parallel injection only

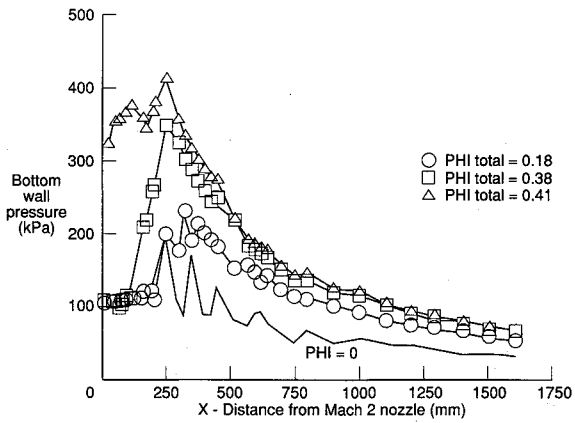

b) Swept ramp injector—configuration II, perpendicular injection only

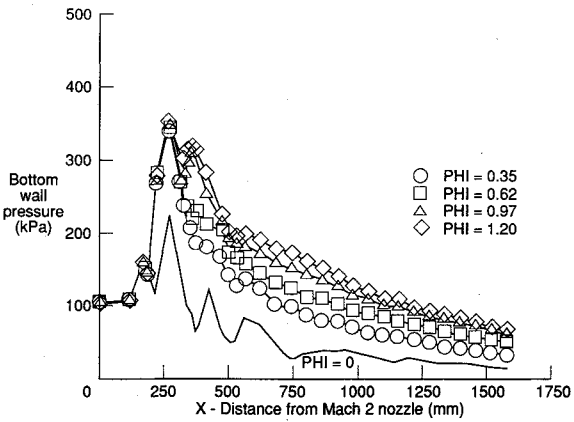

c) Swept ramp injector—configuration III, parallel injection only

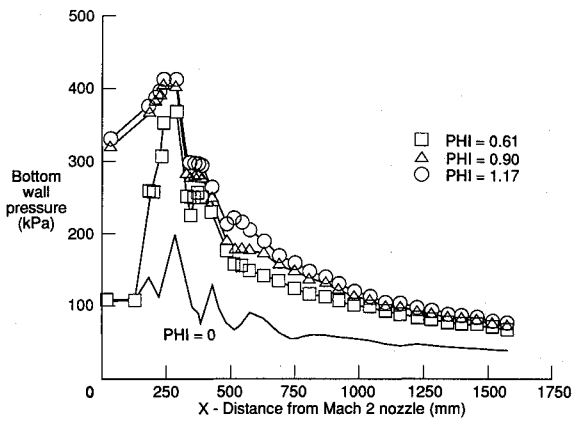

d) Swept ramp injector—configuration III, parallel and perpendicular injection

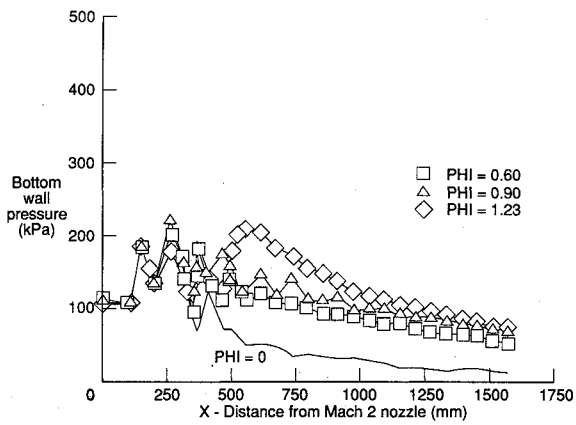

e) Unswept ramp injector—configuration III, parallel injection only

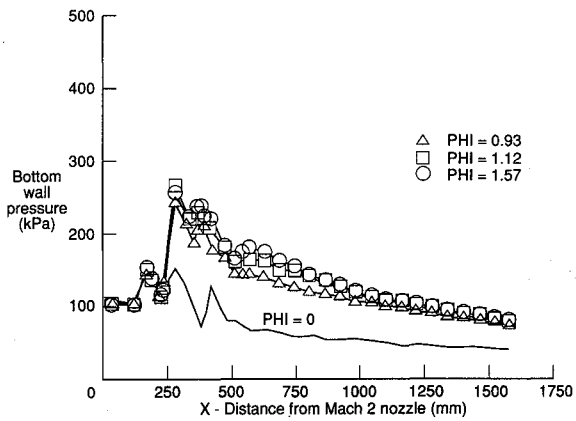

f) Unswept ramp injector—configuration III, parallel and perpendicular injection

Fig. 5 Typical centerline pressure distribution, $M_1 = 2$, $TT = 1700$ K, $P_{heater} = 793$–800 kPa.

5) A one-dimensional multistep integration of the governing equations was performed using COMBAN.[11] This one-dimensional analysis code uses the experimental pressure distribution, the test gas and fuel flow rates, and the computed static properties entering the combustor to calculate a fuel reaction distribution that is consistent with the measured data. The analysis does not account for oblique shock waves that cause losses and nonuniform pressure distribution. The one-dimensional analysis technique is used for making a comparative assessment of tests in similar hardware. Test results were compared using the following computed parameters: average pressure rise $P/P0$, combustion efficiency η_c, and Mach number M.

Test Results

Flow Visualization Tests

A series of shadowgraphs were taken and typical results are shown in Fig. 4 for different test conditions: no fuel injection, parallel fuel injection, and simultaneous, parallel and, perpendicular injection (the flow is from right to left). The pictures shown here are for the swept ramp injector configuration and the pressures downstream of the injectors are near ambient (open-duct tests). The clearance between the reflected oblique shock wave and the ramp apex is about 5–6 mm (taken from the pictures in Fig. 4), which verified the predicted clearance, 5.84 mm. Pressure distributions along the upper wall perpendicular to the flow direction at three cross sections indicated an almost uniform lateral distribution and verified the assumption of a planar oblique shock wave. Figure 4b illustrates the flowfield when fuel is injected from the swept ramp injectors. The fuel injection is overexpanded due to near ambient pressure at the injection zone. The free shear layer at the end of the ramp clearly indicates the mixing and the reaction zone. Figure 4c illustrates the simultaneous injection of fuel from both the parallel and the perpendicular injectors. Adding perpendicular injection displaces the free shear layer toward the upper wall. The parallel injection zone is the same as in Fig. 4b. It was indicated by UV-TV that combustion occurred in the region of the parallel injectors at both test conditions.

Duct Configuration Tests

Tests were conducted in a wide range of fuel/air equivalence ratios and a total temperature range of 1400–2200 K. During the test program, fuel injection, upstream interaction limits, autoignition limits, and combustor performance were monitored. These performance parameters are discussed.

Pressure Distribution in the Duct

About 140 pressure taps were installed on each duct configuration. Pressure distributions were recorded on the injector model and the top, bottom, and side walls along the entire length of the duct. Typical pressure distributions, along the centerline of the bottom wall at a total temperature of about 1700 K are presented in Fig. 5. Pressure distributions across the injector block will be discussed for each duct configuration. In each graph, a pressure distribution is presented at $PHI = 0$ as a reference for the pressure rise due to combustion. It should be noted that an average pressure at each axial station was used for calculating combustion efficiency. Because of the presence of oblique shocks in the duct, the average pressure distribution sometimes differed from that shown for the bottom wall, centerline distribution.

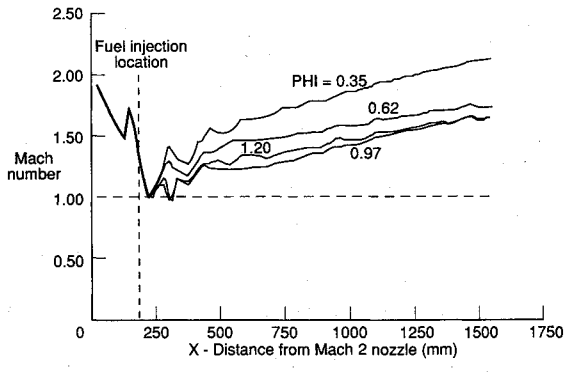

Fig. 6 Typical Mach number distribution.

Since configuration I could only be operated at very low PHI without upstream interaction, due to the constant area duct downstream, no results are shown for this case.

Pressure distributions along the duct for tests with duct configuration II are shown in Figs. 5a and 5b. Shock wave locations when $PHI = 0$ can be clearly observed. The peaks in this curve indicate oblique shock waves reflected from the bottom wall due to the ramps on the injector block. Since there were limited number of pressure taps, the exact location of the waves have not been recorded. With injection and combustion, the strength of the shock waves in the duct diminished. The pressure rise in the duct was very high even for the low equivalence ratios.

Upstream interaction is defined as the condition where the pressure at the exit of the heater nozzle (i.e., combustor entrance) becomes greater than that observed in the case with no fuel. For the conditions presented in Fig. 5, upstream interaction was indicated when a pressure greater than 350 kPa occurred at an X location of approximately 250 mm along the bottom wall. In Fig. 5a, the pressure distribution for $PHI = 0.44$ indicated a limiting pressure for upstream interaction. In Fig. 5b, the curve for $PHI = 0.41$ indicated upstream interaction when the fuel was injected perpendicular to the air. This similar sensitivity indicates that the swept ramp was an effective mixer and flame holder even when the fuel was not injected from the base.

Pressure distributions along the duct for tests with duct configuration III and swept ramp injectors are shown in Fig. 5c. Shock waves for $PHI = 0$ are similar to that explained above for duct configuration II. The peak pressure rise is almost the same for all the equivalence ratios tested. The pressure peak remained at or below 350 kPa for the entire range of PHI tested. At $PHI > 0.97$, a shock wave is observed at a distance of about $X = 330$ mm. This shock is due to the change in the duct divergence angle from 3 to 2 deg. Between the distances of $X = 150$ mm and $X = 230$ mm, a pressure rise existed along the centerline of the bottom wall. This pressure rise upstream of the fuel injection location indicates a coupling between the downstream combustion induced pressure rise through the recirculation zone created by the swept ramp injectors. The upstream extent of the pressure rise appeared to be limited by the small step at the ramp origin (see Fig. 1). Pressure distributions on the top wall across from the ramps, measured at three cross sections, indicated a nearly uniform distribution, as was observed with the open-duct tests. A nonuniform pressure distribution was measured across the bottom wall at approximately 38 mm upstream of the injector edge. The ramp pressure was lower than the measured pressure on the injector block centerline at this axial location.

Pressure distributions along the duct for tests with duct configuration III and swept ramp injectors combined with perpendicular injection are shown in Fig. 5d. By adding the perpendicular fuel injection, the pressure level in the injector block section increased by about 70 kPa. As can be seen in the figure, the higher pressure levels resulted in upstream interaction at $PHI \geq 0.90$ (for $TT = 1700$ K). A pressure rise between the injector ramps was also observed.

Pressure distributions along the duct for tests with duct configuration III and unswept ramp injectors are shown in Fig. 5e. The pressure along the model and the 3 deg expansion duct was lower in comparison with the swept ramp injector block. This is attributed to a weaker vortical structure associated with the unswept ramps. The pressure peak, at only about 210 kPa, and allowed for a wide range of injected fuel equiv-

alence ratios without upstream interaction. A decreasing pressure was observed on the centerline of the bottom wall, which indicated the lack of back flow between the ramps. This was contrary to that observed with the swept ramp injector configuration. For $PHI = 1.23$, ignition delay was observed and the pressure rise due to combustion occurred downstream of the injector ramps in the expansion duct at approximately $X = 520$ mm.

Pressure distribution along the duct for tests with duct configuration III and unswept ramp injectors combined with perpendicular injection are shown in Fig. 5f. By adding the perpendicular injection to the parallel, the pressure level in the injector block section increased by about 60 kPa, yet it remained well below the rise required for upstream interaction. Furthermore, the addition of perpendicular injection significantly reduced the ignition delay that was witnessed with unswept ramp injection alone.

Mach Number Distribution in the Duct

Mach number along the duct was computed by the one-dimensional COMBAN program. Because the input data to the program was the average pressure distribution, the Mach number computed is the average value at each cross section. Typical results for configuration III with swept ramp injectors are shown in Fig. 6. For many of the duct and fuel injection configurations, the flow reached $M = 1$ downstream of the fuel injection station due to thermal compression and oblique shocks. From the injector block geometry (Fig. 1), it can be seen that the computed sonic flow occurs near the end of the short constant-area duct just downstream of the ramps. By starting the expansion directly after the fuel injection station, bulk supersonic flow may be maintained throughout the duct. At high fuel equivalence ratios, a second calculated sonic condition occurred in the duct (see Fig. 6) at the station where the duct divergence changes from 3 to 2 deg. As previously stated, oblique shock waves occur at this station, and a reduction in the Mach number is expected. The one-dimensional code, of course, does not have oblique shock capturing capability.

Upstream Interaction

Tests with duct configuration I (Fig. 3) and swept ramp injectors resulted in upstream interaction at almost any equivalence ratio and total temperature tested. When the fuel was injected perpendicular to the flow direction with the constant-area duct downstream of the injector block, upstream interaction occurred as *PHI* was increased to 0.12. The upstream interaction in this duct configuration resulted from rapid mixing and good combustion and the resultant pressure rise. As a result of these first tests, an isolator, or constant-area, section was located between the facility nozzle and the injector block. A 2-deg divergent duct was added to interface the injector block to the 1.22-m duct without a rearward-facing step. The swept ramp injectors, even without fuel injection, were effective in enhancing mixing for the perpendicular injection. Previous tests[12] with the rearward-facing step configuration were operated at higher *PHI* without upstream interaction.

In tests with duct configuration II (see Fig. 3) and swept ramp injectors, the maximum equivalence ratio before upstream interaction occurred was about 0.31 and 0.60 at total temperatures of 1400 and 2000 K, respectively. Similar results were also found when adding perpendicular injection to the parallel injection from the swept ramps. Perpendicular-only fuel injection from the swept ramp injector block was more sensitive to upstream interaction than the parallel-only mode of injection in the otherwise identical configuration.

In duct configuration III (Fig. 3), tests with both the swept and unswept ramp injectors indicated different upstream interaction limits. Tests with fuel injection from the swept ramp injector were conducted with an equivalence ratio range up to 1.5 without observing upstream interaction. With the swept ramp injector at the lowest total temperature tested (1400 K), autoignition did not occur for equivalence ratios above $PHI = 0.30$. Tests with parallel injection above fuel equivalence ratios of 1.50 have not been conducted, due to limits in fuel supply pressure with this parallel injector throat size.

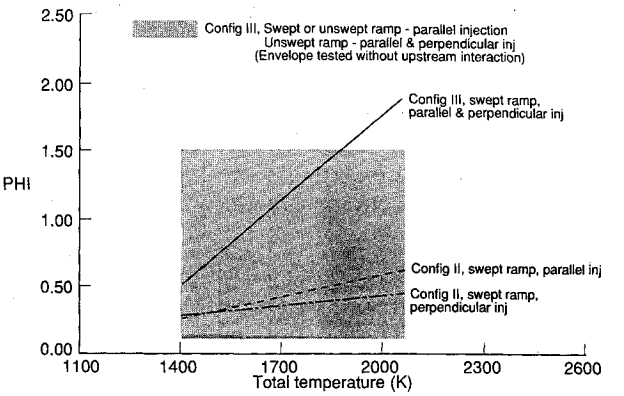

Fig. 7 Summary of upstream interaction data.

Duct configuration III and the swept ramp injector, with both parallel and perpendicular injection, resulted in a limiting value for *PHI* without upstream interaction. This limit, found to be strongly dependent on total temperature, varies from about $PHI = 0.6$ at 1400 K up to $PHI = 1.75$ at 2000 K. This configuration produced autoignition over the entire range of total temperatures and *PHI* values tested.

The unswept ramp injector block was tested in duct configuration III in order to obtain a performance comparison with the swept ramp injector model. High-temperature tests with the unswept ramp injectors were conducted with an equivalence ratio range up to 1.5 without observing upstream interaction. At $TT = 1400$ K and $PHI = 1.50$, a limit of upstream interaction was observed.

Duct configuration III and the unswept ramp injector with both parallel and perpendicular injection resulted in lower limiting *PHI* values than noted with the parallel injection only. This limit was about 0.60 at 1400 K total temperature. For all other test temperatures up to 2050 K and *PHI* up to 1.5, upstream interaction was not observed.

A summary of the upstream interaction limits for the different duct configurations and injector types is shown in Fig. 7.

Combustion Efficiencies

Combustion efficiency was calculated using a one-dimensional analysis program, COMBAN, with the average pressure at each station (see data analysis procedure mentioned earlier). The reacted fuel equivalence ratio ϕ_r is related to the combustion efficiency ϕ_t by

$$\eta_c = \phi_r/\phi_t \tag{1}$$

The unreacted fuel is assumed to be in thermal equilibrium with the combustion products at the local average static conditions. To compare the computed efficiencies with a reference efficiency distribution, the mixing model "recipe" was chosen.[13] The following formula predicted the mixing distribution vs the nondimensionalized distance downstream for perpendicular and parallel fuel injection. The "recipe" is valid for sonic injection from both walls of a two-dimensional duct, with the spacing between fuel injectors being equal to the gap G between the walls and the fuel injector diameter $d = G/15$. The length required for complete mixing, X_l, when the injected equivalence ratio is unity is

$$X_l = 60\ G \tag{2}$$

The length required for complete mixing, X_ϕ, is given by

$$X_\phi/X_l = 0.179\ e^{1.72\phi}, \qquad \phi < 1 \tag{3}$$

$$X_\phi/X_l = 3.333\ e^{-1.204\phi}, \qquad \phi > 1 \tag{4}$$

The mixing efficiency η_m is defined by

$$\eta_m = 1.01 + 0.176\ \ell n\ (X/X_\phi) \tag{5}$$

for perpendicular injection and

$$\eta_m = X/X_\phi \tag{6}$$

for parallel injection.

If the fuel injection angle is between 0 and 90 deg, the mixing efficiency can be interpolated linearly between the parallel and perpendicular values. Computed combustion efficiencies and mixing model efficiencies as a function of fuel equivalence ratio *PHI* are shown in Fig. 8. For reference, the mixing model efficiency is shown in Fig. 8 for the perpendicular (A) and parallel (B) injection equations given above. Computed combustion efficiencies in the ducts at X = 584 mm or 7.6G from the parallel fuel injectors are presented in Fig. 8.

The fuel injection in the tests was from one wall only, and, therefore, the gap used to calculate mixing model efficiencies should be twice the gap in the test (G = 76.7 mm).

Combustion efficiencies calculated with duct configuration II and fuel injection from the swept ramp injector are shown in Fig. 8a. The results are for different total temperatures, yet there was no discernible differentiation in the calculated combustion efficiency. Due to the upstream interaction limits observed with this configuration, the data are limited to *PHI* = 0.6. Efficiencies were not calculated for conditions that resulted in upstream interaction. The computed efficiencies are in good general agreement with those predicted by the perpendicular mixing model. This result indicates that, for the swept ramp injector configuration, the fuel mixing was similar to the mixing predicted for perpendicular sonic injection.

Combustion efficiencies calculated with duct configuration III and swept ramp injectors are shown in Fig. 8b. The results are for different total temperatures from 1400 to 2050 K. Two main observations from these data are as follows:

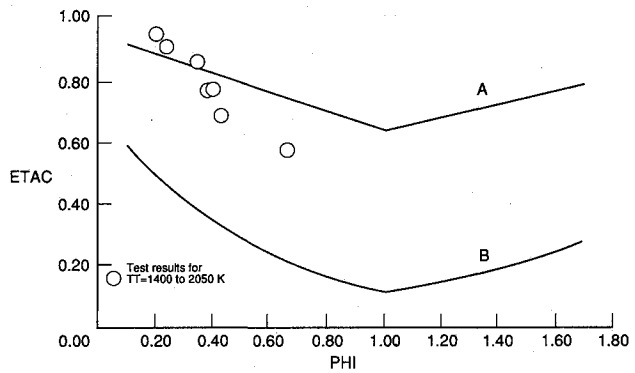

a) Swept ramp injector—configuration II, parallel injection only

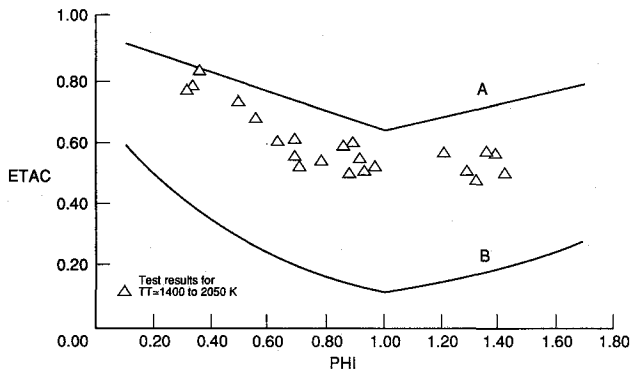

b) Swept ramp injector—configuration III, parallel injection only

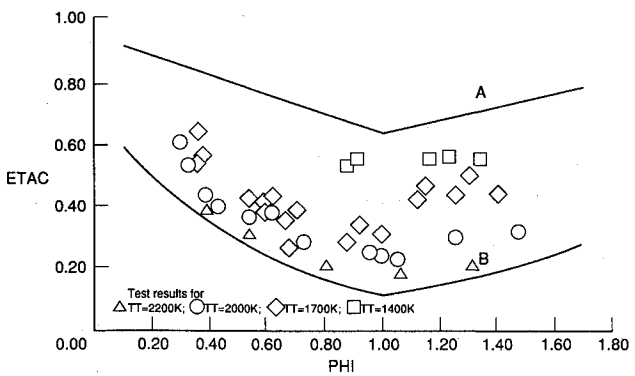

c) Unswept ramp injector—configuration III, parallel injection only

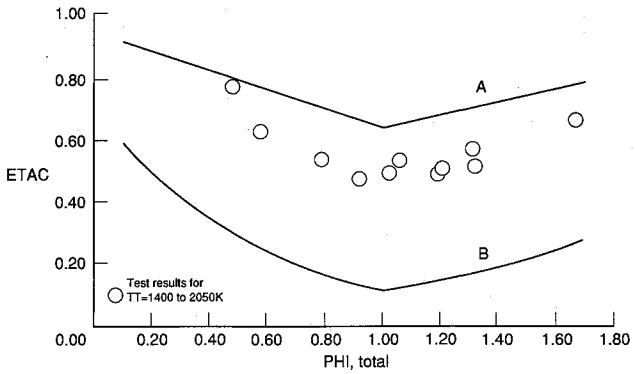

d) Swept ramp injector—configuration III, parallel and perpendicular injection

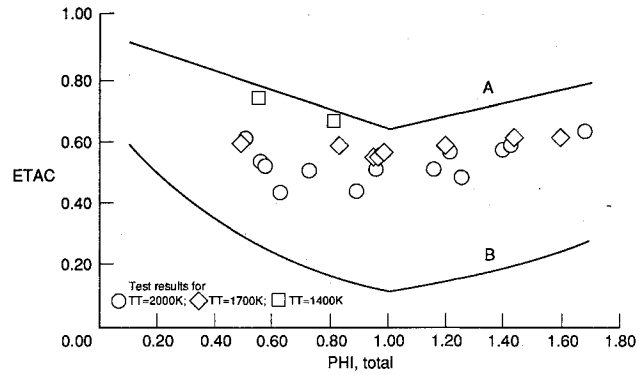

e) Unswept ramp injector—configuration III, parallel and perpendicular injection

Fig. 8 Computed combustion efficiency at 7.6 gaps: A, mixing model for perpendicular sonic injection; B, mixing model for parallel sonic injection.

Table 1 Combustion efficiency at $X/G = 7.6$

Injector type	$PHI = 0.5$	$PHI = 1.0$	$PHI = 1.2$
Perpendicular mixing model	0.80	0.65	0.69
Parallel mixing model	0.29	0.13	0.16
Swept ramp-parallel injection	0.69	0.51	0.54
Unswept ramp-parallel injection	0.47	0.32	0.47
Swept ramp-parallel injection combined with perpendicular injection	0.73	0.50	0.52
Unswept ramp-parallel injection combined with perpendicular injection	0.64	0.55	0.60

1) Computed combustion efficiency as a function of *PHI* is similar to the perpendicular sonic injection mixing model, in spite of the almost parallel injection in this configuration.

2) The computed combustion efficiency is not dependent on facility total temperature.

Combustion efficiencies calculated with duct configuration III and unswept ramp injectors are shown in Fig. 8c. The results are for different total temperatures from 1400 to 2200 K. The following can be observed from these data:

1) Computed combustion efficiencies as a function of *PHI* tend toward the parallel injection mixing model.

2) Combustion efficiency is dependent on total temperature. As the temperature increases, the efficiency decreases. The largest temperature influence is at $PHI > 1$. The temperature dependence described here may be explained by the shortened residence time and the increased velocity of the test gas at higher total temperatures.

Combustion efficiencies for duct configuration III and the swept ramp injector with both parallel and perpendicular injection are shown in Fig. 8d. The results are for different total temperatures from 1400 to 2050 K. The results shown are very similar to those observed with parallel injection only from the swept ramp injector. Adding perpendicular injection had little effect on the calculated combustion efficiency.

Combustion efficiencies calculated for duct configuration III and the unswept ramp injector with both parallel and perpendicular injection are shown in Fig. 8e. The results are for different total temperatures from 1400 to 2200 K. In this case, the perpendicular injection increased combustion efficiencies markedly and resulted in a correlation close to the perpendicular mixing model. Furthermore, with this fuel injection configuration, the temperature dependence was reduced.

As a summary of this section, Table 1 presents typical combustion efficiencies for the different injector types with duct configuration III at a nominal total temperature of 1700 K.

Summary and Conclusion

An experimental study has been conducted to explore techniques to enhance mixing in a scramjet combustor with wall-mounted downstream fuel injection. Two injector models with swept and unswept ramps were designed and tested.

The injector ramp angle was 10.3 deg to yield a reflected shock wave from the duct top wall such that it passed just downstream of the ramp injectors. Fuel injection was at a Mach number of 1.7. Perpendicular fuel injection was added at a location downstream of the parallel fuel injection station to evaluate the performance of combined fuel injection. Direct-connect tests have been conducted with a vitiated heater over a total temperature range of 1400–2200 K. The heater was operated at about 795 kPa to yield atmospheric pressure at the exit of the Mach 2 nozzle. During the runs, fuel was injected from the parallel injectors, from the perpendicular injectors, or from both injectors simultaneously. Unducted flow visualization tests were conducted using the shadowgraph and UV-TV methods.

Three duct configurations were tested with the above fuel injection types. Test results were analyzed by using a one-dimensional scramjet analysis code to convert the pressure distributions and air and propellant mass flows to calculated combustion efficiency and other flow parameters. The following conclusions were drawn:

1) Shadowgraphs verified predicted ramp shock location.

2) UV-TV indicated that combustion occurred in the base region of the ramp injectors.

3) Spontaneous ignition was achieved in all the tests at temperatures above 1400 K. Ignition limit was observed for the swept ramp injector with only parallel injection on duct configuration III, at 1400 K total temperature and *PHI* above 0.30.

4) Tests conducted with a 100-mm-long constant-area section downstream of the swept ramp injector block (configuration I) resulted in upstream interaction at very low equivalence ratios.

5) Relocating a constant-area duct upstream as an isolator (configuration II) increased the upstream interaction limit to about $PHI = 0.35$.

6) Increasing the expansion just downstream of the injector block to 3 deg divergence on both walls (73.2 mm), followed by 2 deg expansion on both walls (1.22 m), allowed a further increase in the equivalence ratio while maintaining supersonic combustion. Maximum *PHI* before upstream interaction with this configuration (III) was above 1.5 for both the swept and unswept ramp injectors. Similar results were observed with the unswept ramp injector with both parallel and perpendicular injection.

7) Limits of *PHI* for upstream interaction were found to increase linearly with total temperature for both perpendicular injection and parallel injection using the swept ramp injector block (configuration III).

8) Calculated one-dimensional Mach numbers in the duct indicated that the flow reached Mach 1 in the short constant-area section on the parallel injector block. Starting the expansion duct immediately downstream of the injection station would probably keep the flow supersonic.

9) Combustion efficiencies achieved with the swept ramp injectors were higher in comparison with those achieved with the unswept ramp injectors.

10) Calculated combustion efficiencies for the swept ramp injector configuration were close to the calculated values for the perpendicular sonic injection mixing model and are not dependent on total temperature. The calculated combustion efficiencies for the unswept ramp injectors were close to the calculated values for the parallel sonic injection model and found to be dependent on stream total temperature, especially for $PHI > 1$.

11) Perpendicular fuel injection combined with fuel injection from the swept ramp injector had no effect on the combustion efficiency. However, perpendicular fuel injection combined with fuel injection from the unswept ramp injector improved the efficiency.

12) Overall, the swept ramp injector design explored here appears to provide good flameholding and enhanced mixing for downstream wall injection. In fact, combustion performance achieved for downstream injection with the swept ramp injector nearly equals the mixing performance expected from perpendicular injection predicted by an empirical mixing correlation. Also, divergence in the duct downstream of the swept ramp injector was effective in controlling upstream interaction for a wide range of equivalence ratios and total temperatures without quenching combustion. Techniques need to be developed to address the total pressure loss associated with the downstream injector types and how the losses increase with increasing Mach number.

References

[1]Northam, G. B., Greenberg, I., and Byington, C. S., "Evaluation of Parallel Injector Configurations for Supersonic Combustion," AIAA Paper 89-2525, July 1989.

[2]Guy, R. W., and Mackley, E. A., "Initial Wind Tunnel Tests at Mach 4 and 7 of a Hydrogen-Burning, Airframe-Integrated Scramjet," NASA Paper 79-8045, 4th International Symposium on Air Breathing, Lake Buena Vista, FL, April 1–6, 1979.

[3]Guy, R. W., Torrence, M. G., Muller, J. N., and Sabol, A. P., "Initial Ground Facility Tests at Mach 7 of a Hydrogen-Burning, Airframe-Integrated Scramjet-Engine Model," NASA TM 84644, 1983.

[4]Andrews, E. H., Jr., Northam, G. B., Torrence, M. G., and Texler, C. A., "Mach 4 Tests of a Hydrogen-Burning, Airframe-Integrated Scramjet," *18th JANNAF Combustion Meeting, Vol. IV,* edited by Debra Sue Eggleston, CPIA Pub. 347, Oct. 1981, pp. 87–96.

[5]Marble, F. E., Hendricks, G. J., and Zukoski, E. E., "Progress Toward Shock Enhancement of Supersonic Combustion Process," *Proceedings: Vol. III, U.S. Contributions, United States-France Joint Workshop on Turbulent Reactive Flows,* Purdue University, West Lafayette, IN, July 1987.

[6]Menon, S., "Shock Waves for Enhanced Mixing in Scramjet Combustors," NASP CR-1028, Dec. 1988.

[7]Metwally, O., Settles, G., and Horstman, C., "An Experimental Study of Shock Wave/Vortex Interaction," AIAA Paper 89-0082, Jan. 1989.

[8]Guirguis, R. H., "Mixing Enhancement in Supersonic Shear Layers: III. Effect of Convective Mach Number," AIAA Paper 88-0701, Jan. 1988.

[9]Swithenbank, J., Eames, I., Chin, S., Ewan, B., Yang, Z., Cao, J., and Zhao, X., "Turbulence Mixing in Supersonic Combustion Systems," AIAA Paper 89-0260, Jan. 1989.

[10]Ames Research Staff, "Equations, Tables, and Charts for Compressible Flow," NACA Rept. 1135, 1953.

[11]Anderson, G. Y., and Gooderum, P. B., "Exploratory Tests of Two Strut Fuel Injectors for Supersonic Combustion," NASA TN D-7581, 1974.

[12]Diskin, G. S., and Northam, G. B., "Sensitivity of Supersonic Combustion to Combustor/Flameholder Design," *ICAS Proceedings 1988,* Vol. 1, AIAA, Washington, DC, 1989, pp. 58–66.

[13]Northam, G. B., Anderson, G. Y., "Supersonic Combustion Ramjet Research at Langley," AIAA Paper 86-0159, Jan. 1986.